

Ion diagnostics with rf probes in a warm magnetoplasma

W. T. C. Grimson* and K. G. Balmain

Department of Electrical Engineering, University of Toronto, Toronto, Canada M5S 1A4
(Received 10 June 1974)

The admittance of a parallel-plate capacitor immersed in a warm collisional electron-ion magnetoplasma is studied both experimentally and theoretically. Particular attention is given to the admittance behavior near the lower-hybrid resonance. It is shown that this resonance can be identified experimentally, and therefore that admittance measurements can be used to measure the ion plasma frequency directly, in magnetoplasmas containing one predominant ion species.

I. INTRODUCTION

The behavior of the admittance of rf probes in plasmas is significant in relation to ion diagnostics in ionospheric and laboratory plasmas. In single-ion or multi-ion magnetoplasmas a resonance called the lower-hybrid resonance (LHR) plays an important role in ion diagnostics.¹ The LHR has been identified in ionospheric quadrupole-probe mutual-impedance measurements,² mutual-impedance measurements being advantageous because the effect of inhomogeneities around the probes is minimized.³ VLF self-admittance measurements on a dipole have been carried out in the ionosphere on international satellites for ionospheric studies (ISIS),⁴ and this paper is addressed in part to the problem of interpreting such ionospheric measurements, approaching the problem by studying the closely related admittance problem of parallel-plate probes in a laboratory magnetoplasma.

In the laboratory experiment to be described, the probes are given a dc bias with respect to the plasma, and this bias is shown to be significant. In theory, an absorptive boundary condition^{5,6} is used to simulate the use of a small positive dc bias to bring the probes from near-floating to near-collapsed-sheath conditions. Some calculations were also done using a vacuum-gap-sheath model with a purely reflective boundary condition, a representation which has been studied extensively.⁷

II. THEORY

The quantity to be calculated is the admittance per unit area of a capacitor formed by two infinite parallel plates separated by $2l$ and immersed in a magnetoplasma as shown in Fig. 1. The derivation of the admittance formula is straightforward⁸ and is presented here in abbreviated form.

A. Basic equations

A warm electron-ion plasma with a static magnetic field B_0 imposed is considered. The time variation as assumed is $\exp(j\omega t)$. The linearized force equation is written

$$j\omega m \mathbf{v} = q\mathbf{E} + q\mathbf{v} \times \mathbf{B}_0 - (\gamma kT/N_0)\nabla n - m\nu \mathbf{v}, \quad (1)$$

where m is the particle mass, \mathbf{v} is the particle velocity, q is the charge, \mathbf{E} is the electric field, n is the particle number density above ambient N_0 , T is the particle temperature, and ν is the collision frequency. The subscripts i and e denote ions and electrons, respectively. Poisson's equation is used with the quasistatic assumption

$$\nabla \cdot \mathbf{E} = (n_i - n_e)q/\epsilon_0 \quad (2)$$

$$\mathbf{E} = -\nabla\phi,$$

where ϵ_0 is the permittivity of free space and ϕ is the potential. The magnetic field is given as

$$\mathbf{B}_0 = \hat{z}B_0. \quad (3)$$

From the geometry of Fig. 1, it is seen that the field quantities are functions of x only, and thus

$$\mathbf{E} = \hat{x}E_x = -\hat{x}\frac{\partial\phi}{\partial x}. \quad (4)$$

The velocities are assumed to be in the x direction. The spatial variation is assumed to have the form $\exp(-jkx)$ for the purpose of calculating the longitudinal-wave dispersion relation which is derived from Eqs. (1)–(4) and has the form

$$\det \begin{bmatrix} -\alpha_1 & \beta_1 \\ \alpha_2 & -\beta_2 \end{bmatrix} = 0, \quad (5)$$

where

$$\alpha_1 = \frac{N_0 e^2}{m_e \epsilon_0} = \omega_{pe}^2,$$

$$\alpha_2 = \frac{k^2 \gamma_i k T_i}{m_i} + \frac{N_0 e^2}{m_i \epsilon_0} - \omega^2 + j\omega \nu_i + \frac{e^2 B_0^2 / m_i^2}{1 - j\nu_i / \omega},$$

$$= k^2 a_i^2 + \omega_{pi}^2 - \omega^2 + j\omega \nu_i + \frac{\Omega_i^2}{1 - j\nu_i / \omega}, \quad (6)$$

$$\beta_1 = k^2 a_e^2 + \omega_{pe}^2 - \omega^2 + j\omega \nu_e + \frac{\Omega_e^2}{1 - j\nu_e / \omega},$$

$$\beta_2 = \omega_{pi}^2.$$

Note that the definitions of ω_p , a , and Ω are implicit in Eq. (6).

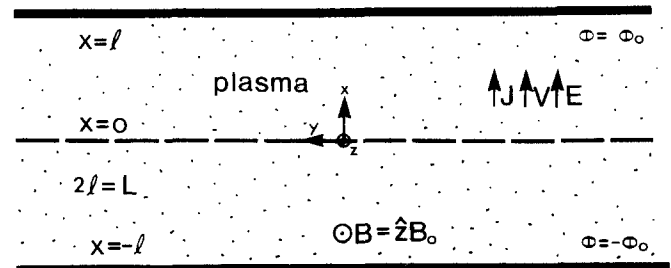


FIG. 1. Parallel-plate plasma capacitor.

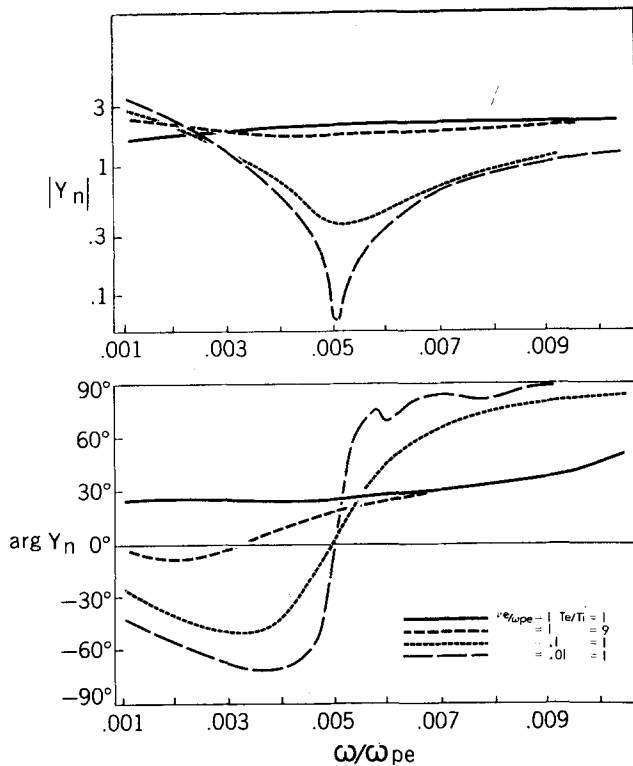


FIG. 2. Admittance magnitude and phase for various collision frequencies. $\lambda_e = 0.1$ cm, $\Omega_e/\omega_{pe} = 10$, $L = 1.4$ cm, $\omega_{pi}/\omega_{pe} = 0.005$, $p_e = 0$, and $p_i = 1.0$.

Equation (5) results in four values of k , two of those values representing waves propagating in the positive x direction and designated by k_1 and k_2 (having $\text{Im}\{k\} < 0$). With $\omega_{pe} \gg \omega_{pi}$ and $\omega_{pi} \gg \Omega_e$, the two frequencies ω_{LHR} and ω_{UHR} (the lower-hybrid and upper-hybrid frequencies) are resonant frequencies of the dispersion relation and are given by

$$\begin{aligned} \omega_{LHR} &= \omega_{pi} (1 + \omega_{pe}^2/\Omega_e^2)^{-1/2}, \\ \omega_{UHR} &= \Omega_e (1 + \omega_{pe}^2/\Omega_e^2)^{1/2}. \end{aligned} \quad (7)$$

Note that for $\Omega_e \gg \omega_{pe}$, the LHR approaches ω_{pi} and the UHR approaches Ω_e .

B. Admittance calculation

A number of different models have been used to represent the sheath region.⁹ The absorptive boundary condition is used here to describe, approximately, a thinly sheathed probe,⁵ and a variable absorption coefficient is used to represent, approximately, the effect of varying the probe bias between floating and collapsed-sheath conditions,⁶ while ignoring plasma inhomogeneity. The potential boundary conditions are

$$\phi(l) = \phi_0, \quad \phi(-l) = -\phi_0. \quad (8)$$

The absorptive boundary conditions are

$$\begin{aligned} v_\alpha(l) &= g_\alpha n_\alpha(l), \\ v_\alpha(-l) &= -g_\alpha n_\alpha(-l), \end{aligned} \quad (9)$$

where

$$\alpha = e, i, \quad a_\alpha^2 = \frac{\gamma K T_\alpha}{m_\alpha}, \quad g_\alpha = P_\alpha \frac{a_\alpha}{N_0} \left(\frac{2}{\pi}\right)^{1/2}. \quad (9')$$

The quantity P_α is the surface absorption coefficient for the α species, with a value of unity approximately representing full particle absorption and a value of zero representing complete reflection. The excess number density of charged particles is given by

$$n_\alpha(x) = C_\alpha \exp(-jkx). \quad (10)$$

From the basic equations it can be shown that

$$C_i/C_e = \beta_1/\alpha_1 = \beta_2/\alpha_2. \quad (11)$$

Two parameters, λ_1 and λ_2 , are introduced¹⁰ such that

$$\lambda_1 = \frac{C_i}{C_e} \Big|_{k=k_1} \quad \text{and} \quad \lambda_2 = \frac{C_i}{C_e} \Big|_{k=k_2}. \quad (11')$$

Therefore, the following expressions can be written for $n_e(x)$ and $n_i(x)$:

$$\begin{aligned} n_e(x) &= A \cos(k_1 x) + B \sin(k_1 x) + C \cos(k_2 x) + D \sin(k_2 x), \\ n_i(x) &= \lambda_1 [A \cos(k_1 x) + B \sin(k_1 x)] + \lambda_2 [C \cos(k_2 x) + D \sin(k_2 x)]. \end{aligned}$$

Poisson's equation is now used to give $E(x)$. From it, two integrations give $\phi(x)$ which contains terms of the form $Gx + H$, where G and H are constants of integration. The potential boundary conditions now determine that $A = C = H = 0$, and G is arbitrarily set equal to unity (which has the effect of fixing the applied voltage). The linearized equation of motion and the absorptive boundary conditions determine the remaining two constants B and D . The input admittance is given by

$$Y = A_p Y_0 = A_p (J_p + J_d) / (-2\phi_0), \quad (12)$$

where

$$\begin{aligned} J_p &= N_0 e (v_i - v_e), \\ J_d &= -j\omega \epsilon_0 \frac{d\phi}{dx}, \end{aligned}$$

and A_p is the probe area. With $\alpha_e = N_0 g_e$ and $\alpha_i = N_0 g_i$, the input admittance per unit area can be written in the form

$$\begin{aligned} Y_0 &= \left\{ j\omega \left[\left(\frac{\lambda_1 - 1}{k_1} \right) B \cos(k_1 l) + \frac{\lambda_2 - 1}{k_2} D \cos(k_2 l) + 1 \right] \right. \\ &\quad \left. + [B(\alpha_e - \lambda_1 \alpha_i) \sin(k_1 l) + D(\alpha_e - \lambda_2 \alpha_i) \sin(k_2 l)] \right\} \\ &\quad \left\{ \frac{2}{\epsilon_0} \left[\left(\frac{\lambda_1 - 1}{k_1^2} \right) B \sin(k_1 l) + \left(\frac{\lambda_2 - 1}{k_2^2} \right) D \sin(k_2 l) + l \right] \right\}^{-1}. \end{aligned} \quad (13)$$

In the calculations to follow, the admittance plotted is the normalized quantity $Y_n = Y_0 / \pi \epsilon_0 f_{pe}$, where f_{pe} is the electron plasma frequency expressed in Hz. Another quantity appearing in the graphs is λ_e which is essentially the Debye length and is defined by $\lambda_e = a_e / \omega_{pe}$.

C. Numerical results

A typical set of admittance calculations is shown in

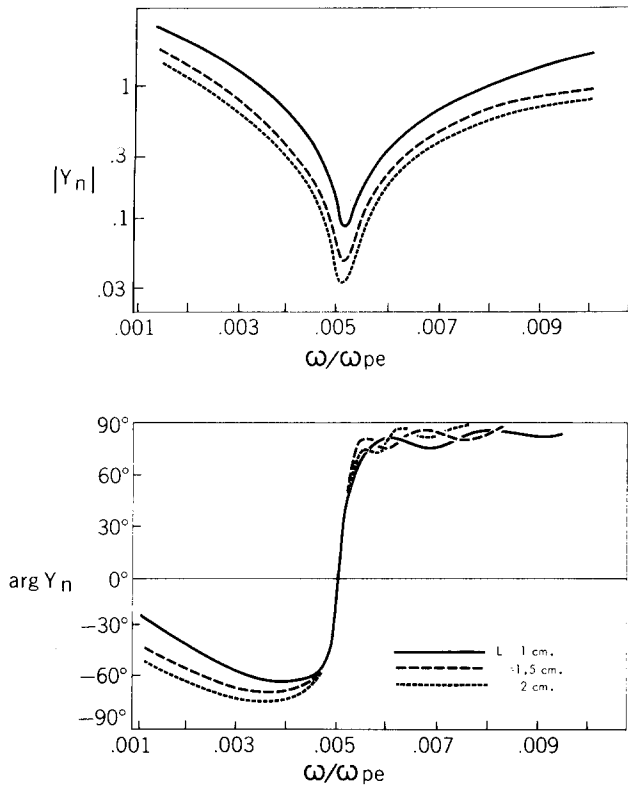


FIG. 3. Admittance magnitude and phase for various spacings. $\lambda_e = 0.1$ cm, $\Omega_e/\omega_{pe} = 10$, $\nu_e/\omega_{pe} = 0.01$, $\omega_{pi}/\omega_{pe} = 0.005$, $T_e/T_i = 1$, $p_e = 0$, and $p_i = 1.0$.

Fig. 2 for the case of a high magnetic field and consequently a lower-hybrid resonance which is close to the ion plasma frequency. The resonance in the admittance is within 3% of the LHR, and an increasing collision frequency shifts the resonance frequency appreciably only for $\nu_e/\omega_{pe} > 0.1$. Reduction of the ion temperature brings the resonance closer to the LHR. In Fig. 3, the resonance frequency is seen to be unaffected by probe spacing, suggesting that the resonance is a property of the medium rather than of the probe geometry. An interference pattern can be seen just above the LHR in the phase graph, an effect due to the excitation of small-amplitude short-wavelength longitudinal waves.^{2,11}

Similar calculations (not shown) were carried out for $\Omega_e/\omega_{pe} = 1$, and the resonance near the LHR was found to vary in frequency by $\pm 5\%$ with variations in probe spacing; the sharpness of the resonance was also reduced. At zero magnetic field a broad resonance was also observed but its frequency was found to be highly dependent on probe spacing, therefore being of little use for diagnostics and probably difficult to observe in non-ideal geometries. For all finite values of magnetic field the principal admittance resonance was found to approach the LHR more closely as the ion temperature was lowered. At zero magnetic field the nature of the admittance resonance was found to be highly dependent on the values chosen for the surface absorption coefficients, but for the cases already mentioned of moderate and high magnetic fields, variations in the absorption coefficients had negligible effect on the resonance in the vicinity of the LHR. The calculations shown make use of the absorption coefficients $p_e = 0$ and $p_i = 1$, repre-

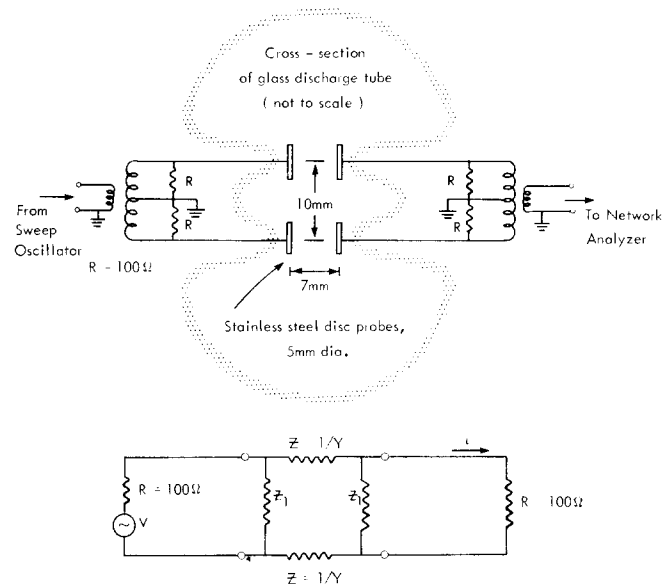


FIG. 4. Experimental arrangement and equivalent circuit.

senting a thin sheath which reflects most of the electrons but permits the ions to pass through to the electrode where they are absorbed. The nonzero value for p_i gives an admittance phase of zero in the zero-frequency limit and damps out resonances at frequencies below the LHR. Nonzero values of p_e represent a lowering of the sheath potential barrier to electrons, but such values are not useful for representing a large positive bias which produces plasma depletion and plasma inhomogeneity. The introduction of a vacuum-gap region adjacent to the probe surface to represent negative bias tended mainly to reduce the amplitude of the admittance resonance.

III. EXPERIMENTAL RESULTS

The experiments were carried out in a cold-cathode cylindrical discharge tube 8 cm in diameter and 11 cm in distance between the cathode and anode, which were both stainless steel and grooved for greater effective area. For each sequence of experiments the discharge tube was evacuated, baked, backfilled with neon, and sealed. Such a procedure gives excellent short-term repeatability in the experiments, although the pressure inside the tube falls slowly due to the self-pumping action of the discharge. The axial magnetic field was provided by an external solenoid.

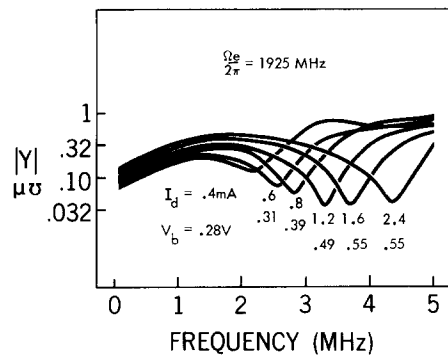


FIG. 5. Variation of the minimum in admittance magnitude with discharge current I_d . In each case the optimum bias voltage V_b is given.

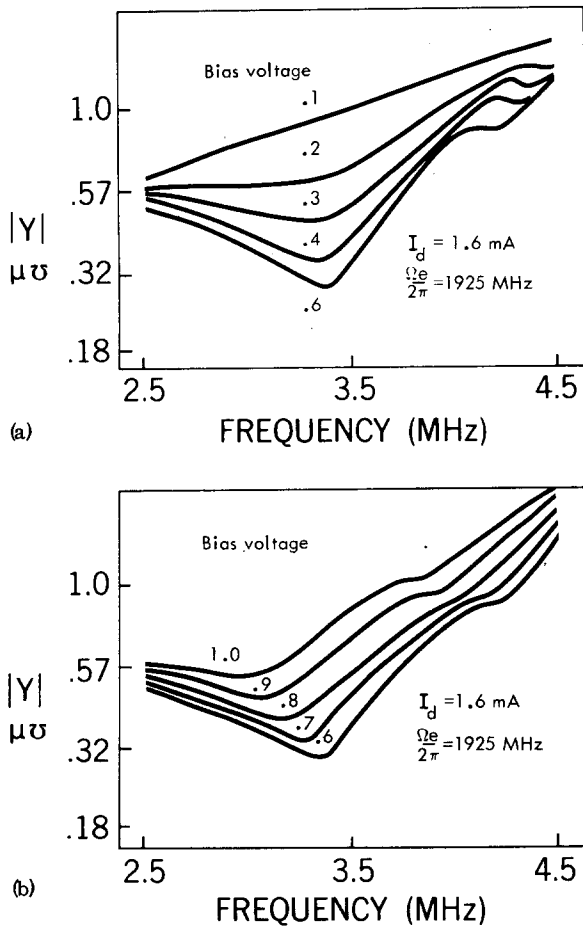


FIG. 6. Bias effects on admittance near LHR using expanded frequency scale. (a) The effect of a negative bias change from optimum (b) The effect of a positive change.

The basic measurement geometry is shown in Fig. 4 and can be seen to involve transmission between two pairs of parallel-plate disk probes. Because the impedances Z and Z_1 (which are of the order of $1\text{ m}\Omega$) are much higher than the input source or load impedances, the quantity measured is the ratio of load current to input voltage, or mutual admittance. Furthermore, it can be seen from the equivalent circuit that for this case the quantity measured is essentially proportional to the self-admittance Y between facing probes. It is important to note that the probes are geometrically and electrically balanced, so that no rf conduction current flows in the anode and cathode leads, and negligible rf displacement current flows between the body of the plasma and adjacent conductors; unbalanced experiments of this type failed because of stray capacitance, anode rf currents, and the influence of the anode sheath.

Figure 5 shows typical admittance magnitude characteristics observed for the balanced probes. The admittance minimum moves up in frequency as the discharge current increases in a manner which is consistent with the notion that the resonance is the LHR.

The indicated dc bias of the probes is with respect to the anode, and the effect of varying the bias is found to be crucial in determining the sharpness of the resonance. Figure 6 shows the variation of the admittance magnitude minimum with bias, using an expanded fre-

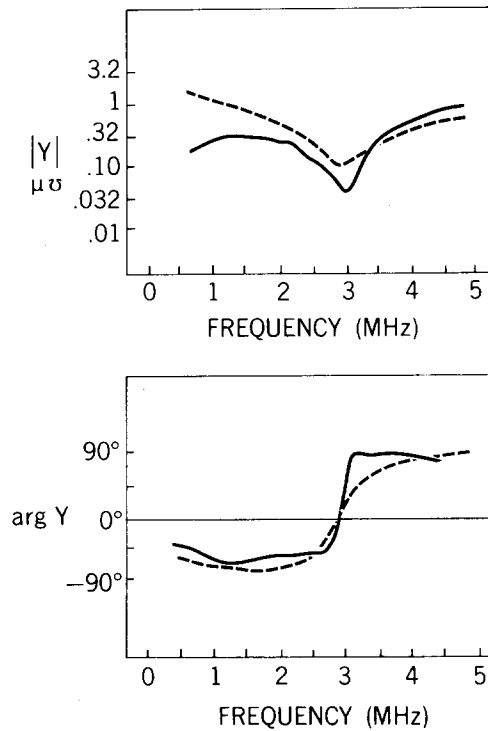


FIG. 7. Comparison of measured admittance (solid lines) and calculated admittance (dashed lines). $I_d = 1\text{ mA}$, $\Omega_e/2\pi = 1925\text{ MHz}$, $V_b = 0.4\text{ V}$, $f_{pe} = 600\text{ MHz}$, $f_{pi} = 3\text{ MHz}$, $\nu_e = 6\text{ MHz}$, $T_e = 1010\text{ K}$, $T_i = 335\text{ K}$, $p_e = 0.01$, $p_i = 1.0$, and $L = 7\text{ mm}$.

quency scale. The sharpest resonance occurs for a small positive bias of 0.6 V , which would produce a thin sheath region. Making the bias more positive lowers the resonant frequency slightly, presumably because of plasma depletion, while making the bias more negative expands the sheath and adds enough capacitive reactance to remove the resonance. Generally speaking, bias variations weakly influence the resonance frequency but strongly influence the occurrence of the resonance.

Figure 7 shows the calculated admittance of the parallel-plate capacitor compared directly with measured values for a typical case. The values of the plasma parameters inserted into the admittance computer program were provided by various diagnostic measurements carried out along with the main admittance experiment. Langmuir probes,¹² resonance

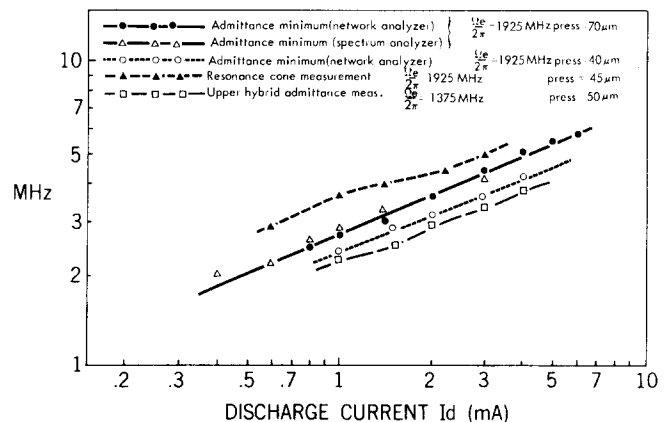


FIG. 8. Lower-hybrid frequency (ion plasma frequency) measured using various techniques.

cones,^{13,14} and microwave measurements of the UHR¹⁵ were used independently to find electron density and temperature variations with discharge current.

Figure 8 shows a summary of one complete set of measurements in which the frequency of the admittance magnitude minimum is plotted against discharge current. In one case the sweep generator and network analyzer were replaced with a spectrum analyzer and tracking generator, to show that the measurements were independent of the instrumentation used. The ion plasma frequencies deduced from the cone resonance and microwave determination of the UHR are also plotted for various discharge currents. The observed resonance and the LHR frequency are found to be generally the same, within experimental error estimates.

IV. CONCLUSIONS

Swept-frequency measurement of plasma probe admittance can be used to identify the lower-hybrid frequency when the magnetic field is high enough (so that the electron gyro frequency is approximately equal to or higher than the electron plasma frequency). This measurement is especially convenient for measuring ion density when the magnetic field is high enough so that the lower-hybrid frequency is approximately equal to the ion plasma frequency (for a single predominant ion species). It is important to note that the probe bias must be adjusted to bring the probes close to but still less than plasma potential. In laboratory situations, admittance measurements of the type described are usually easier to perform than mutual impedance measurements. In space plasma situations, adjusting probe bias is often neither convenient nor possible, and the effective probe bias is determined by factors such as spacecraft orientation and velocity. This explains in part why usable spacecraft antenna admittance measurements of the lower-hybrid frequency are rare events.¹⁶

ACKNOWLEDGMENT

The authors thank R. E. Barrington and F. H. Palmer for helpful discussions related to this work. The research was supported by the Communications Research Centre, Department of Communications, Canada, under Department of Supply and Services Contract No. DSS 36100-4-0235. Permission by the Department of Communications to publish the results of this study is acknowledged. Support was also provided by the National Research Council of Canada.

*Present address: Ferranti Ltd., Robertson Ave., Edinburgh EH11 1PX, Scotland.

¹R. E. Barrington, in *Plasma Waves in Space and in the Laboratory*, Vol. 1, edited by J. O. Thomas and B. J. Landmark (Elsevier, New York, 1969), p. 361; Proc. IEEE 57, 1036 (1969).

²C. Beghin and R. Debrie, J. Plasma Phys. 8, 287 (1972).

³L. R. O. Storey, M. P. Aubry, and P. Meyer, in *Plasma Waves in Space and in the Laboratory*, Vol. 7, edited by J. O. Thomas and B. J. Landmark (Elsevier, New York, 1969), p. 303.

⁴C. D. Florida, Proc. IEEE 57, 867 (1969).

⁵K. G. Balmain, Radio Sci. 1, 1 (1966).

⁶B. Homonick and K. G. Balmain, Can. J. Phys. 51, 513 (1973).

⁷P. E. Vandenplas, A. M. Messiaen, J. -L. Monfort, and J. J. Papier, Plasma Phys. 12, 391 (1970).

⁸W. T. C. Grimson, M. A. Sc. thesis (University of Toronto, 1973) (unpublished).

⁹T. R. Kaiser and J. K. E. Tunaley, Space Sci. Rev. 8, 32 (1968).

¹⁰A. F. Aleksandrov, Sov. Phys. -Tech. Phys. 10, 24 (1965); 10, 185 (1965).

¹¹T. Aso, Planet. Space Sci. 22, 583 (1974).

¹²I. G. Brown, A. B. Compher, and W. B. Kunkel, Phys. Fluids 14, 1377 (1971).

¹³R. K. Fisher and R. W. Gould, Phys. Fluids 14, 857 (1971).

¹⁴K. G. Balmain, Electron. Lett. 9, 312 (1973).

¹⁵J. M. Chasseriaux, R. Debrie, and C. Renard, J. Plasma Phys. 8, 231 (1972).

¹⁶R. E. Barrington and F. H. Palmer (private communication).